Determination of Weighting Functions for Energy-Weighted Acquisition

Raymond P. DeVito and James J. Hamill

Applied Physics and Research Group, Siemens Gammasonics, Inc., Hoffman Estates, Illinois

Energy-weighted acquisition (EWA) is an image filtering technique, with a different spatial filter (weighting function) for each energy. The imaging characteristics of EWA are governed by the weighting functions used during the acquisition of the image. The determination of weighting functions is more complicated than the determination of energy windows in conventional imaging because the number of degrees of freedom is much greater. A methodology by which weighting functions can be produced is described. The weighting function is determined by minimizing a generalized chi-square with variable contributions from coefficients quantifying key image characteristics, e.g., signal-to-noise ratio, spatial resolution, and scatter fraction. Varying the importance of these characteristics gives us a workable function-generation tool, able to address a variety of clinical needs. The resulting weighting functions exhibit good scatter reduction properties at various scatter depths, as demonstrated by measurements of line source response functions in a scattering medium at depths from 5 to 14 cm. Energy weighting can also be used to compensate for collimator penetration from high energy gamma rays. Weighting functions are tested in the laboratory using both planar and SPECT phantoms.

J Nucl Med 1991; 32:343–349

Energy-weighted acquisition (EWA) involves a fundamental change in the way data is utilized for gamma ray imaging (*1,2*). EWA reduces the effects of Compton scattering, the principal image degradation mechanism of nuclear imaging (*3–5*). It is here that EWA provides the greatest contribution to image quality. Energy weighting can also reduce the effects of high energy penetration through the collimator (*1*), a common problem for isotopes like iodine-123 (*6*), which has high energy contaminant gamma rays in addition to the 159 keV gamma ray used in imaging. More generally, since EWA is a flexible image filtering technique, with a different spatial filter (weighting function) for each energy, total system performance can be improved and advantageously matched to the desired imaging goals. The energy windowing technique, used by gamma cameras before EWA, is a simple form of energy weighting, in which all weights are either 0 or 1. Beck (*7,8*) suggested that the event weight should, ideally, change gradually from positive to negative values in going from the high energy side of the normal window towards lower energies. This work details the methodology by which the weighting functions used in clinical and phantom imaging (*1,2,5*) were produced.

The energy weighting technique requires weighting functions that produce good results under realistic imaging conditions. To determine a viable weighting function, it is necessary to deal with the greatly increased number of degrees of freedom that become accessible with the transition from simple windows. We no longer deal with a small number of energy window widths and centroids, but rather with several spatial distribution parameters for each of many 1-keV wide energy bins. The performance characteristics of the gamma camera must be considered in conjunction with the physics of Compton scattering in clinically realistic environments. Image characteristics must be quantified in ways that allow representation of a variety of system response criteria. The point response is used as a flexible computational base to incorporate the essential physical attributes needed to derive general purpose weighting functions.

THEORY

Data produced by even the best instruments are flawed by the imperfect response of the instrument and by interference from the local environment. We consider a geometry in which the gamma camera is in the x′,y′ plane, with the patient above that plane, at positive z′ coordinates (*2*). The gamma camera's output is described by the energy-dependent point spread function (EPSF), P(x-x′,y-y′,E,z′), which relates the flux of events out of the gamma camera to the distribution of activity in the patient. We assume that P(x-x′,y-y′,E,z′) is shift-invariant; that is, a function of x-x′ and y-y′, but not x′, y′, x, and y, separately. The variables x′, y′, and z′ are the coordinates of points within the patient, d(x′,y′,z′) is the distribution of radioactivity, and x, y,

Received Nov. 15, 1989; revision accepted Aug. 14, 1990.

For reprints contact: Raymond P. DeVito, Siemens Gammasonics, Inc., Applied Physics and Research Group, 2501 N. Barrington Rd., Hoffman Estates, IL 60195-7372.

and E are the measured camera coordinates of detected events and the energy signal of detected events (keV). The flux of events detected by the gamma camera, $\phi(x,y,E)$, is related to the actual distribution of radioactivity, $d(x',y',z')$, by

$$\phi(x,y,E) = K \int dz' \int dx' \int dy' \; P(x-x',y-y',E,z')\, d(x',y',z'), \quad \text{Eq. 1}$$

where K is a normalization factor.

The final image, I(X,Y), is built from the gamma camera output, $\phi(x,y,E)$. EWA utilizes an energy-dependent spatial filtering operator, operating on the output of the gamma camera to produce the final image. The final image, I(X,Y), is given by:

$$I(X,Y) = C \int dx \int dy \int dE\; \phi(x,y,E)\; w(X-x,Y-y,E). \quad \text{Eq. 2}$$

The weighting function, w(X-x,Y-y,E), embodies knowledge about the instrument response and the local environmental factors, e.g., Compton scattering. The factor C accounts for the instrumentation and study parameters that link the final image to the input flux, e.g., study duration and pixel size. An important special case is a point source of unit strength with a distribution that may be described as a Dirac delta function:

$$d_{point}(x',y',z') = \delta(x')\delta(y')\delta(z'). \quad \text{Eq. 3}$$

Substituting the point distribution, Equation 3, into the relation for the output of the gamma camera, Equation 1, we have

$$\phi_{point}(x,y,E) = K \int dz' \int dx' \int dy' \; P(x-x',y-y',E,z')\delta(x')\delta(y')\delta(z'), \quad \text{Eq. 4}$$

$$\phi_{point}(x,y,E) = K\; P(x,y,E). \quad \text{Eq. 5}$$

The image of this point source is by definition the point spread function, $p_w(X,Y)$, which is a convolution of the EPSF and the weighting function:

$$p_w(X,Y) = K \int dx \int dy \int dE\; w(x-x,Y-y,E)\; P(x,y,E). \quad \text{Eq. 6}$$

The objective here is to find a well-behaved function which satisfies Equation 6 such that: $p_w(X,y) \approx$ no scatter point source image. Important considerations in seeking a solution are that statistical noise is minimized, the response is stable against energy variations in the camera, and the output is valid over an appropriate range of scatter depth.

METHOD

Measurement of the EPSF

Function generation begins with a measurement of the EPSF for each isotope and for each collimator for which weighting functions are sought. We collect signals from a gamma camera that is viewing a point-like source at position $(X_0, Y_0) \equiv (0,0)$ embedded in a scattering medium. The EPSF depends on z', since this variable effects the spatial resolution of the collimator, and the scattered radiation. In our weighting function determination, we utilize data from a single scatter depth. We investigated the use of EPSFs from multiple scatter depths, but found that the use of a single depth provided weighting functions that had good scatter removal over the range of scatter depths applicable to clinical imaging (*1,2*). The energy response of the gamma camera is first calibrated by exposing the camera to the gamma rays of the three isotopes americium-241, cobalt-57, and barium-133; or alternatively thallium-201, technetium-99m, and gallium-67. The energy resolution is checked and the gamma camera pulse-height (Z) to energy (E) relation is derived (*9*). The spatial resolution and distance scale (cm/pixel) is measured with a pencil-beam cobalt-57 source.

Event-by-event list mode acquisition of data from a point source of activity is acquired. The point source is centered in the field of view of the gamma camera and is embedded in scattering material (Plexiglas) with scatter material both in front of the source (between the camera and the source) and behind the source. Centering the point source in the field of view is an acceptable approximation of general imaging conditions since variations in camera response over the useful field of view are small enough to be insignificant. About 10^7 events are recorded on magnetic storage tape for subsequent analysis. To form the EPSF in polar coordinates (origin directly over the point source), each event is analyzed and assigned to pixels (r,Z) where $r = \sqrt{X^2 + Y^2}$. After all events are processed, the pixel data are normalized to counts/cm^2. Finally, the pulse height data are transformed to absolute energy (in keV) using the measured Z to E calibration. When weighting functions derived from this data are used for imaging, the energy response of the imaging camera will be similarly calibrated so that it also produces an absolute energy scale (*2*). The excellent intrinsic spatial resolution and linearity of modern gamma cameras allows reliable transport of weighting functions between camera systems that are calibrated to absolute energy. Figure 1 shows an isometric plot of the EPSF for ^{67}Ga, imaged with a medium-energy, parallel-hole collimator and at a scatter depth of 7 cm.

Generalized Chi-square

To calculate weighting functions, we must establish clear and mathematically definable imaging goals. We wish to reproduce the same point source image whether or not a scattering medium or other background is present. With the EPSF measured, Equation 6 could be directly solved to determine w(X-x,Y-y,E). Such a solution, however, is unacceptable due to the lack of constraint on image noise and important detector system parameters. Instead of solving the linear relation of Equation 6, we pose a minimization problem involving a few important parameters with adjustable coefficients to control their relative contributions. This control will allow the minimization to produce solutions with a good balance of imaging characteristics. This situation is analogous to collimator selection where sensitivity is traded off relative to resolution to meet the desired imaging goals.

Ideally, the solution we seek is one that produces a point response in scatter resembling the point response with no

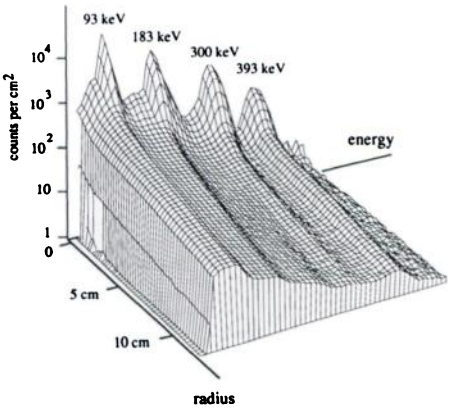

FIGURE 1
Energy-dependent point source response function for gallium-67 at 10 cm scatter depth. The point source response is plotted over the entire energy range used in function generation for this isotope.

background. The background could be composed of, for example, scattered events or events from higher energy gamma rays that penetrate the collimator. The image noise should be minimized, and the noise characteristic needs to be balanced against improvements in scatter content (Fig. 2). The weighting function must be well behaved for energy variations typical of the actual detector and with respect to the amount of scatter material. A weighting function producing good results only over a small range of scatter depths would be unacceptable in the clinical environment where the scatter depths are largely unknown.

We measure the degree of correspondence to the ideal solution with a chi-square-like resolution term which we add to a generalized chi-square parameter, Q, with adjustable coefficients, a_X, a_N, a_S, to balance the importance of resolution, noise, and stability, respectively:

$$Q = a_X\chi^2 + a_N N^2 + a_s S^2. \qquad \text{Eq. 7}$$

PSFs with various weighting functions (gallium-67)

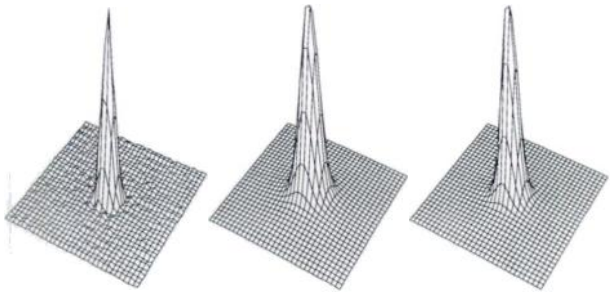

FIGURE 2
Point response functions for various weighting functions for gallium-67 exhibiting good resolution but increased pixel noise, less pixel noise but poor resolution, and an intermediate function exhibiting acceptable noise and resolution.

The terms χ^2, N^2 and S^2 are defined below. This parameter is constructed so that smaller values of Q represent better imaging characteristics.

The resolution term is

$$\chi^2 = \int\int dXdY\ (p_w(X,Y) - p_{ideal}(X,Y))^2 f_x(X,Y), \qquad \text{Eq. 8}$$

where $p_w(X,Y)$ is the PSF with EWA described by Equation 6 and $p_{ideal}(X,Y)$ is the desired PSF with realistic resolution for the collimator and detector (e.g., PSF with a point source and no scatter). The function $f_x(X,Y)$ alters the importance of different radii of the point image. A simple but useful radial dependance is $f_x(X,Y) = r^b$, where $r = \sqrt{X^2 + Y^2}$. With this formulation, as b becomes larger, the tails of the point image influence χ^2 more. In clinical imaging, the distribution of interest is usually degraded by the scatter background from neighboring regions. The magnitude of this effect can be modified to control the impact of extended source distributions. We found that b = 1 incorporates the influence of the distance scatter tails to a degree that is approximately the same as clinical applications.

The manifestations of statistical noise must be acceptable if the weighting function is to be useful. The noise in an EWA image is more complicated than simple Poisson noise (*7*). It is a function of the scatter depths and the activity in the neighboring region. We define a measure of the statistical noise for our test point source as

$$N^2 = \int dE\ W(E)^2\ P'(E). \qquad \text{Eq. 9}$$

In this expression, $W(E)^2$ is the weighting function squared, integrated over space,

$$W(E)^2 = \int\int dx\ dy\ w(x,y,E)^2, \qquad \text{Eq. 10}$$

and P'(E) is the energy spectrum, integrated over space,

$$P'(E) = \int\int dX\ dY\ p(X,Y,E) f_E(X,Y). \qquad \text{Eq. 11}$$

The function $f_E(X,Y)$ serves the same purpose as the function $f_x(X,Y)$ of Equation 8 and is usually of the same functional form. Equation 9 is proportional to the noise variation for a uniform sheet source, if $f_E(X,Y) = r^b$ (as above) with b = 1. A single number that measures the noise in an image cannot completely account for all the noise characteristics associated with an image. This representation is used in deriving weighting functions that have demonstrated good noise properties for planar and SPECT phantoms.

The energy variation from point to point in a modern gamma camera is small, yet energy variations can arise from residual errors in the energy correction mechanisms or from photomultiplier gain variations. The weighting functions should be made insensitive to energy variations on the order of intrinsic camera response (Fig. 3). To guide the weighting function calculation, we define an energy variation measure. Consider the effect of an energy offset on the output of the weighting function. Let

$$S^2 = 1/2(\Delta_+^2 + \Delta_-^2)^2, \qquad \text{Eq. 12}$$

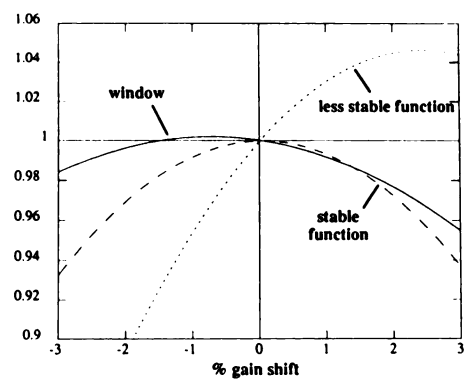

FIGURE 3
Relative counts in the peak of a gallium-67 point source response. Curves for a 15% energy window, a stable weighting function, and a less stable weighting function are plotted as a function of percent gain shift relative to no gain shift.

where $\Delta_{\pm}$ is the response when the energy spectrum is shifted, minus the response with no shift:

$$\Delta_{\pm} = \int\int dX\, dY\, (p_w^{\text{shifted} \pm 1\ \text{keV}}(X,Y) - p_w^{\text{no shift}}(X,Y) \times f_S(X,Y)). \quad \text{Eq. 13}$$

The function $f_S(X,Y)$ is the same as $f_E(X,Y)$ and $f_x(X,Y)$ described above. As the weighting function becomes less sensitive to energy variations, the values of $\Delta_{\pm}$ will decrease.

The weighting function should provide a reduction in scatter content and acceptable imaging characteristics over the range of scatter depths found in the clinic. It is possible to incorporate multiple depths in the generalized chi-square. Alternately, a single representative depth can be used and the resulting weighting function checked afterwards for an acceptable depth dependence. This latter procedure is the one we have chosen, as it is less computationally intensive and experience has shown that the weighting functions we have generated tend to be well behaved with scatter depth. Examples of this dependence are shown below in the experimental verification section.

Gradient Search

A gradient search method (*10*) is used to find a weighting function that minimizes the generalized chi-square defined above. The method is able to handle non-linear constraints and is stable against input data noise. The main problem with this method is that it is a computationally intense, iterative procedure.

In the gradient search procedure, all components of the weighting function are incremented simultaneously. The relative magnitudes are adjusted so that the resultant search pattern is along the direction of maximum variation of the chi-square. The direction of maximum variation is found by computing the gradient, ∇Q:

$$(\nabla Q)_i = \frac{\partial Q}{\partial w_i} \approx \frac{Q(w_i + \Delta w_i) - Q(w_i)}{\Delta w_i}. \quad \text{Eq. 14}$$

We define a dimensionless gradient, γ, with a magnitude of unity:

$$\gamma = \frac{\frac{\partial Q}{\partial w_i}}{\sqrt{\sum_{j=1}^{N} \left(\frac{\partial Q}{\partial w_i}\right)^2}}. \quad \text{Eq. 15}$$

For each step in the search, the weighting function is altered along the direction of steepest descent by

$$w_i \leftarrow w_i - \gamma_i \Delta w_i. \quad \text{Eq. 16}$$

The minus sign above ensures that the generalized chi-square decreases. The starting point for the search is either the standard window function or a previously computed weighting function.

During the weighting function search, two constraints are imposed. First, the normalization of the weighted PSF is required to match that of the standard window PSF. This constraint keeps the number of counts of the weighted image comparable to the response of the standard window, and it inhibits the search routine from seeking out null solutions, for in the generalized chi-square formulation, a null weighting function could produce a favorable chi-squared value by producing a zero noise and stability term. Second, the values for the different components of the weighting function are kept within limits required by the imaging hardware discussed below.

Implementation of Energy-Weighted Acquisition

The EWA technique has been implemented in a pre-processing configuration with dedicated hardware, a weighted-acquisition module (WAM). The WAM processes event information from the camera, and provides a standard image acquisition device with the information necessary to assemble the final processed image (*1,2*). The WAM contains two 128 × 128 pixels, signed, real number "read-add-write" buffer memories that allow it to assemble information used to determine the image value on an event-by-event basis. By using these buffer memories, the WAM processes events with real-valued weighting functions, yet uses unblank pulses (an integer system) for building images. The buffer memory is not used for image display, but only as an intermediate step in the image formation process. It records negative and fractional values, while the image acquisition device records positive integer values. Two simultaneously acquired images, each processed by independent weighting functions, are available from the WAM, providing the opportunity to acquire a weighted image together with a standard window image, or to directly compare two weighting functions.

The spatial template of the weighting function is a 21-pixel kernel (a 5 × 5 region, less four corner pixels) covering an area about 16 mm in diameter when using a 39-cm circular field of view camera. The weighting function is described by four spatial components: one for the central pixel, one for the four side neighbors, one for the four corner neighbors, and one for the 12 pixels forming a ring around these, minus the corners. The weighting function is digitized in energy into 1-keV increments. Figure 4 shows the kernel distribution and a representative weighting function.

For each event, the energy is digitized and the discrete energy value is used as an index for the table of weighting

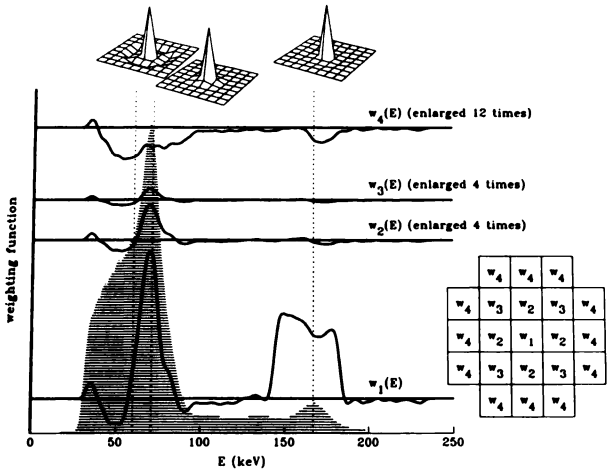

FIGURE 4
Weighting function and spatial kernel used in the weighted acquisition module. The four spatial components of a representative weighting function for thallium-201, along with the corresponding energy spectrum, are shown as a function of energy.

values. The weighting value for the center of the kernel is added to the buffer memory at the event position. The new value is then checked: if it is +1.0 or more, the integer value is removed from memory and converted into a series of one or more unblank pulses, i.e., equal to the net integer value of the event. The position signals from the gamma camera are then transmitted to the image acquisition device with the original coordinates and resolution. The weighting values for the other 20 pixels around the kernel center are added to the corresponding buffer pixels as data for future reference, i.e., when a subsequent event occurs in one of these pixels.

RESULTS

Using the function generation method described above, weighting functions have been calculated for a variety of isotopes and collimators. Our first efforts were concentrated on technetium-99m, thallium-201, and gallium-67. These isotopes provide a range of gamma ray imaging problems. Technetium-99m provides an example of scatter removal from an isotope with only one gamma-ray emission. The influence of the scattering of higher energy emissions into the energy range of lower energy emissions is a major complicating factor for gallium-67. When using thallium-201, the imaging problems associated with broad X-ray emissions are of major concern. The X-rays are composed of several different energy emissions closely spaced so that small angle scattering from higher energies overlap the lower primary energies. For imaging problems that are related to the detected energy spectrum, our methods have proven to be robust enough to effect some improvement (*1,2,5*). Following this initial experience, weighting functions for indium-111, iodine-123, iodine-131, and xenon = 133 were also calculated and validated in phantom and clinical trials.

DISCUSSION

The simplifications incorporated into the generalized chi-square can lead to weighting functions that satisfy the minimization condition, but in some respect are unacceptable for clinical imaging. Unacceptable PSF, unusual noise characteristics, flood nonuniformity, or poorly-behaved scatter depth dependence can occur. A methodology has been developed to systematically check weighting functions for these kinds of behavior. The experimental verification proceeds from simple radioisotope distributions to more complex tomographic applications. Finally, the weighting funtions are validated by testing in the clinic.

Candidate weighting functions should provide a reduction in scatter contribution throughout the range of scatter depths important in clinical imaging (*1*). To verify this, line spread functions (LSF) are measured for a line source of activity (length larger than the gamma camera diameter) positioned behind 5.0, 9.8, and 13.9 cm of soft tissue equivalent scattering material. Figure 5 is an example of comparison of candidate weighting function LSFs and standard windowed LSFs for thallium-201. The candidate weighting function significantly reduces the scatter contribution over this range of scatter depths.

To visualize and to quantify more imaging characteristics of the test weighting functions, image data are acquired for a simple planar phantom (Schramm phantom, Ana Sim, Inc.) and a uniform sheet source, imaged at various depths with Plexiglas interposed as a soft tissue equivalent scattering medium. An example of a Schramm phantom study is shown in Figure 6 for thallium-201, comparing two weighting functions and a standard window image. Profiles through the 100% cold region and through the 100% hot region in the 50% uniform section are presented. If a weighting function fails to produce visually and quantifiably superior images, that weighting function is not considered for clinical testing.

For weighting functions with tomographic application, functions are tested by imaging a SPECT phantom (Data Spectrum Corp.) loaded with 100% cold spheres, hot rods, and a uniform section. Data are acquired in 128 × 128 format and sampled for 128 projections. The test weighting function and a standard window are acquired simultaneously and are backprojected using the same reconstruction filter. The optimal reconstruction filter for the backprojection of the weighting function data is likely to be different than that for the standard windowed data. The same reconstruction filter is used, however, to evaluate the effect of the weighting function compared to the standard window, independent of reconstruction effects. While some weighting

FIGURE 5
Line spread response function for a representative weighting function for thallium-201 at 5.0, 9.8, and 13.9 cm scatter depth. The weighting function is derived from data from a single scatter depth, but is effective at reducing the scatter contribution over a range of scatter depths relevant to clinical nuclear medicine imaging.

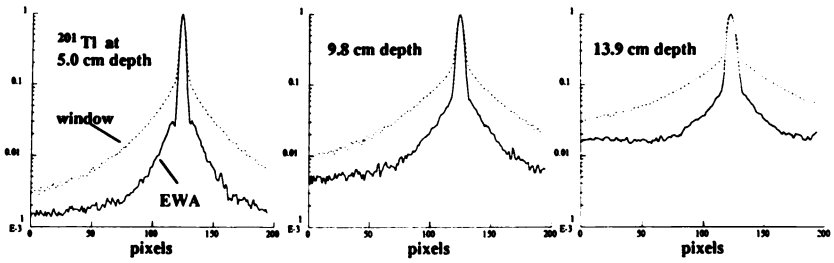

functions perform better for SPECT application than others, in our experience, weighting functions that produce acceptable planar images also produce acceptable SPECT images (*1*,*5*).

When acceptability has been established for the LSF, planar phantom image, and SPECT phantom image, the weighting function is tested in a clinic to evaluate the weighting function's performance for a variety of applications. During this trial, the weighting function is always imaged simultaneously with a standard window image for comparison. Images are evaluated by nuclear medicine physicians for impressions of overall perform-

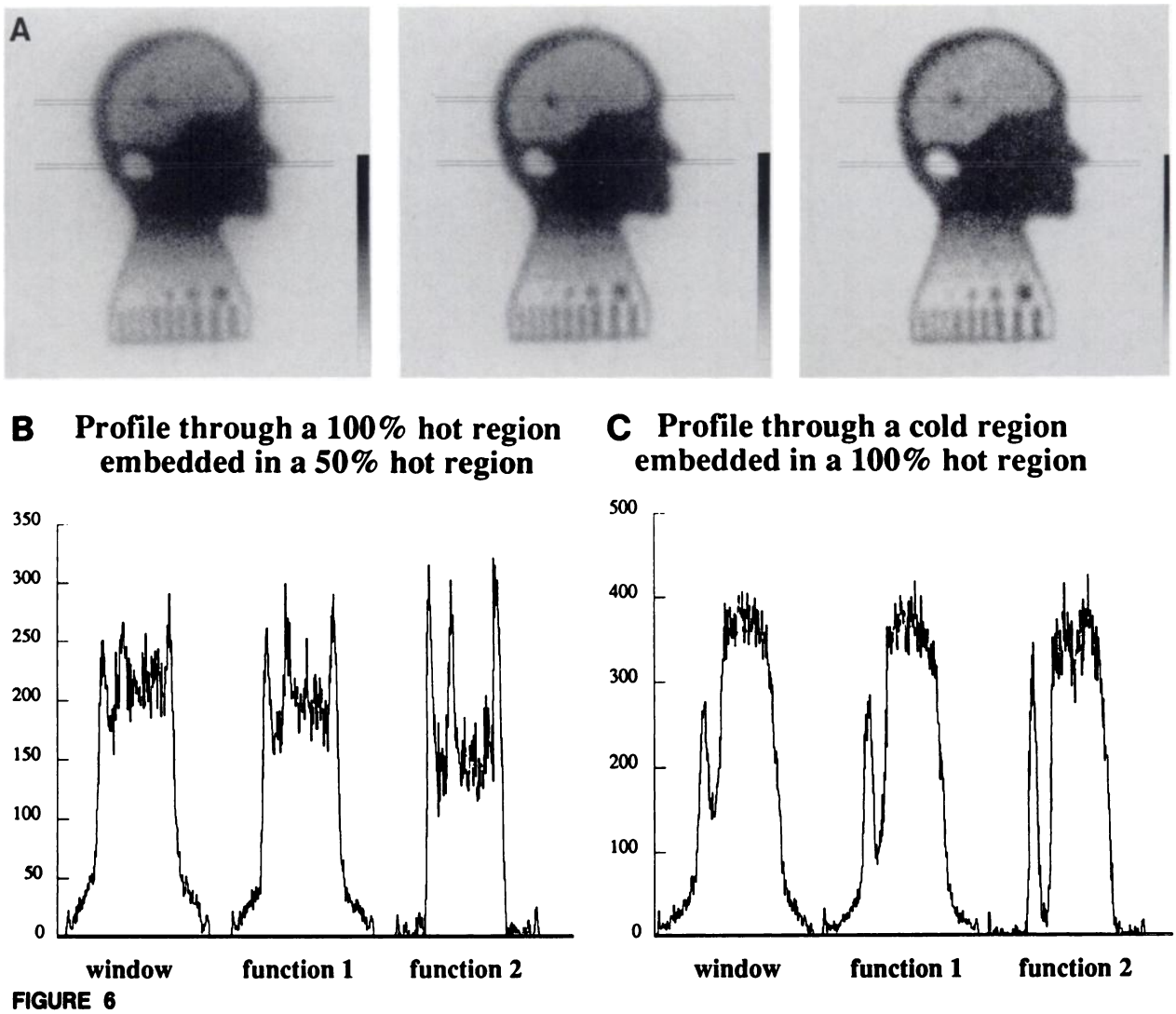

FIGURE 6
Example of performance of two weighting functions for gallium-67. (A) Images of a Schramm phantom imaged with a medium-energy collimator with 7 cm of scatter material. From left to right, the images were acquired using a normal window, weighted acquisition with weighting function 1, and weighted acquisition with weighting function 2. (B) Profiles of the Schramm phantom through a 100% hot region embedded in a 50% hot region, and; (C) cold region embedded in a 100% hot region.

ance and comparison with the standard window images. If the short trial period is successful, a longer study is initiated for evaluation of specific clinical protocols.

REFERENCES

1. DeVito RP, Hamill JJ, Treffert JD, Stoub EW. Energy-weighted acquisition of scintigraphic images using finite spatial filters. *J Nucl Med* 1989;30:2029–2035.
2. Hamill JJ, DeVito RP. Scatter reduction with energy-weighted acquisition. *IEEE Trans Nucl Sci* 1989;NS-36: 1334–1339.
3. Ehrhardt JC, Oberley LW, Lensink SC. Effect of a scattering medium on gamma ray imaging. *J Nucl Med* 1974;15:943–948.
4. Jaszczak RJ, Coleman RE, Whitehead FR. Physical factors affecting quantitative measurements using camera-based single photon emission computed tomography (SPECT). *IEEE Trans Nucl Sci* 1981;NS-28:69–80.
5. Halama JR, Henkin RE, Friend LE. Gamma camera radionuclide images: improved contrast with energy weighted acquisition. *Radiology* 1988;169:533–538.
6. Ziessman HA, Fahey FH, Gochoco JM. Impact of radiocontaminants in commercially available iodine-123: dosimetric evaluation. *J Nucl Med* 1986;27:428–432.
7. Beck RN, Zimmer LT, Charleston DB, Hoffer PB. Aspects of imaging and counting in nuclear medicine using scintillation and semiconductor detectors. *IEEE Trans Nucl Sci* 1972;19:173–178.
8. Beck RN, Zimmer LT, Charleston DB, et al. Advances in fundamental aspects of imaging systems and techniques. In: *Medical radioisotope scintigraphy, volume I.* Vienna: IAEA;1973:3–45.
9. Engelkemeir D. Nonlinear response of NaI(Tl) to photons. *Rev Sci Instr* 1956;27:589–591.
10. Bevington PR. *Data reduction and error analysis for the physical sciences.* New York: McGraw-Hill; 1969;215–219.